



Universiteit
Leiden
The Netherlands

Complete elastic tensor across the charge-density wave transition in monocrystal Lu₅Ir₄Si₁₀

Betts, J.B.; Migliori, A.; Boebinger, G.S.; Ledbetter, H.; Galli, F.; Mydosh, J.A.

Citation

Betts, J. B., Migliori, A., Boebinger, G. S., Ledbetter, H., Galli, F., & Mydosh, J. A. (2002). Complete elastic tensor across the charge-density wave transition in monocrystal Lu₅Ir₄Si₁₀. *Physical Review B*, 66(6), 060106. doi:10.1103/PhysRevB.66.060106

Version: Not Applicable (or Unknown)

License: [Leiden University Non-exclusive license](#)

Downloaded from: <https://hdl.handle.net/1887/76593>

Note: To cite this publication please use the final published version (if applicable).

Complete elastic tensor across the charge-density-wave transition in monocrystal $\text{Lu}_5\text{Ir}_4\text{Si}_{10}$

J. B. Betts, A. Migliori, G. S. Boebinger, and H. Ledbetter

National High Magnetic Field Laboratory, Los Alamos National Laboratory, Los Alamos, New Mexico 87545

F. Galli and J. A. Mydosh

Kamerlingh Onnes Laboratory, Leiden University, 2300 RA Leiden, The Netherlands

(Received 21 June 2002; published 30 August 2002)

We report resonant ultrasound spectroscopy (RUS) measurements of a monocrystal of $\text{Lu}_5\text{Ir}_4\text{Si}_{10}$ from 2 to 300 K. We observe a large, anisotropic hysteretic stiffening of the elastic tensor on cooling below T_{CDW} at 80 K, consistent with a commensurate charge-density wave (CDW), and inconsistent with a second-order phase transition. Therefore, the transition must be first order, and hence coupled strongly to the lattice. Although the c axis is the CDW propagation direction, from RUS it appears that the CDW must derive most of the c -axis modulation by assembling it from lateral charge transfer in the a - b plane.

DOI: 10.1103/PhysRevB.66.060106

PACS number(s): 62.20.Dc, 62.90.+k, 64.70.Kb

$\text{Lu}_5\text{Ir}_4\text{Si}_{10}$ represents a uniquely structured intermetallic compound¹ that possesses a chainlike arrangement of Lu atoms along its tetragonal (and small) c axis. The compound displays a dramatic structurally-related transition at ~ 80 K followed by a superconducting one at 3.9 K.² X-ray diffraction³ was used to observe a weak superstructure peak for (0 0 1) scans appearing sharply at 80 K. This peak was positioned near the value of $3/7$ and was attributed to the formation of a commensurate charge-density wave (CDW). The CDW in $\text{Lu}_5\text{Ir}_4\text{Si}_{10}$ has been studied using specific heat, transport, susceptibility and thermal expansion techniques.³ Each technique has provided evidence for a CDW transition, strongly coupled to the lattice, near 80 K. Here we provide measurements of a key missing property, the adiabatic elastic tensor,⁴ which enables the CDW in this material to be fully characterized.

We report measurements using resonant ultrasound spectroscopy (RUS) of the elastic response of a single crystal of $\text{Lu}_5\text{Ir}_4\text{Si}_{10}$ from 2 to 300 K, with emphasis on the region near the superconducting transition T_c of 3.9 K and the charge density wave transition T_{CDW} at 80 K. With resolution of one part in 10^6 , we observe no discontinuities in the elastic tensor near T_c . In contrast, with resolution of five parts in 10^6 , we observe a large, anisotropic stiffening of the elastic tensor on cooling below T_{CDW} consistent with the predicted² commensurate CDW, and inconsistent with any mean-field second-order phase transition. Together with the observation of hysteresis, the transition must be first order, and hence strongly coupled to the lattice.

Monocrystals were grown in a tri-arc furnace using a modified Czochralski technique. The purities of the starting elements melted in a stoichiometric ratio were Lu:4N, Ir:4N, and Si:5N. Parts of the single crystal were sealed in a quartz tube and annealed at 900 °C for one week. All samples were analyzed by electron-probe microanalysis, which proved them to be single phase (secondary phases <1%) and to have the correct 5:4:10 stoichiometry (within the 1% resolution). A rectangular (3% errors in parallelism and perpendicularity) shaped bar ($0.1345 \times 0.0472 \times 0.1090$ cm³, 6.4 mg) with the c -axis oriented along the short dimension was cut. 20- μ m flaws, caused by spark erosion, were visible. The geometric density was 9.25 g cm⁻³,

reasonable for so small a sample compared to theoretical x-ray-diffraction-computed density of 8.89 g cm⁻³. The orientation of the sample with crystallographic principle axes was within $\pm 2^\circ$. Measurements were performed using a commercial RUS spectrometer.⁵ The process that RUS relies on for determination of moduli from resonances is somewhat complex, requiring a Levenberg-Marquardt inversion procedure applied to a Lagrangian-minimization method for computing resonances from moduli. This procedure applied to data from samples with the relatively large geometric errors described above, typically produces moduli with an absolute accuracy of order 5%, although the technique is capable of accuracies better than 0.03% (Ref. 6) for less flawed crystals. Precision, however, can be one part in 10^6 , especially if moduli are not needed but, instead, discontinuities in mechanical resonance frequencies versus temperature are sought, as in the attempt here to detect the elastic response at the superconducting transition. We used the National High Magnetic Field Laboratory (NHMFL) 15-T He³ system, with calibrated Cernox thermometer within 0.5 cm of the sample in the 1-mB exchange gas. We estimate the error in sample temperature at 80 K to be less than 5 mK. Frequency measurements near the CDW transition had a precision of about five parts in 10^6 , while those near the superconducting transition at 3.9 K had a precision of about one part in 10^6 .

The crystal structure of $\text{Lu}_5\text{Ir}_4\text{Si}_{10}$ is shown in Fig. 1. Note the three Lu and Si sites, while the Ir is single-site specific. This compound provides a good candidate for a charge-density-wave phase transition because: (1) it has a large unit cell (38 atoms), (2) it is quasi-one-dimensional (along c), as required by Peierls⁷; (3) six of seven atomic sites have two degrees of freedom in the ab plane, thus the crystal structure can change without altering either the point group or the space group. Along c , the Lu_1 - Lu_1 interactions provide the unit-cell framework. The compound shows a strong layer structure: alternating A and B layers perpendicular to c . The A layer comprises Lu_1 , Ir, Si_1 , and Si_2 atoms. Layer B comprises Lu_2 , Lu_3 , and Si_3 atoms (no Ir atoms). Iridium's nearest-neighbor atoms are Si_3 , bonded out of the plane. At ambient temperature, we observe (see Table I) $c_{11} = c_{22} \approx c_{33}$, indicating the same compressional stiffness along all three principal axes; in contrast, strong shear an-

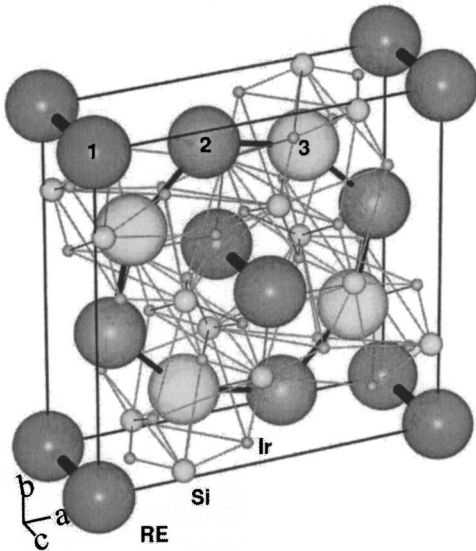


FIG. 1. Crystal structure of Lu₅Ir₄Si₁₀ showing the *a-b* planes and the short chains along the *c* direction. The three different Lu sites are indicated. This strongly 1-D character along *c* is important for the CDW instability to occur.

isotropy appears: c_{66} exceeds $(c_{11} - c_{12})/2$ by 20% and c_{44} by almost 150%. (In a tetragonal crystal structure, $(c_{11} - c_{12})/2$ is the shear stiffness for a wave moving along [110], polarized along $[\bar{1}10]$.) Thus, altering interatomic-bond angles within the *ab* plane (c_{66} is the measure of *ab*-plane shear stiffness) is more difficult than changing bond angles out of the plane (c_{44} is a measure of the out-of-*ab*-plane shear stiffness).

A charge-density-wave transition amounts to altering ion positions and electron distribution so as to form new or stronger bonds.⁷ Hence, as our measurements confirm below, we expect the low-temperature c_{ij} to exceed the extrapolated higher-temperature values. The strong mode-softening that occurs upon cooling toward the charge-density-wave transition is consistent with a mean-field Landau phase-transition theory modified to allow first-order phase transitions.^{7-12,14} Most of the mode softening occurs in $(c_{11} - c_{12})/2$ rather than in c_{44} or c_{66} . A detailed analysis of the effects of c_{66} and $(c_{11} - c_{12})/2$ deformations on bond angles would reveal which in-plane bonds soften during cooling.

Surprisingly, the transition to the commensurate CDW phase does not destroy the mechanical resonances of the

TABLE I. The elastic moduli in GPa just above and just below the CDW transition in Lu₅Ir₄Si₁₀. Absolute error bars are approximately 5% for the diagonal moduli and 25% for the off-diagonal ones, however, relative changes are determined far better (<1%) for the diagonal moduli.

<i>T</i> (K)	c_{11}	c_{33}	c_{23}	c_{12}	c_{44}	c_{66}
76.5	232	229	67	48	55	113
81.5	210	228	65	52	55	108
220	228	224	68	52	54	105
295	226	225	67	51	54	105

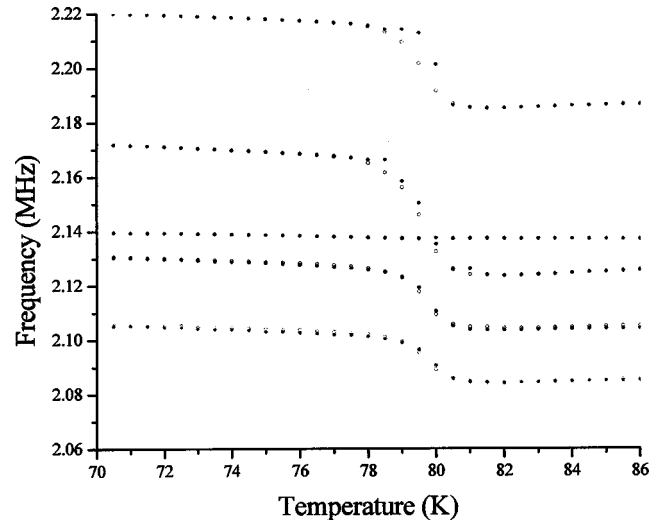


FIG. 2. Some mechanical resonances of a monocrystal sample of Lu₅Ir₄Si₁₀ near the CDW transition. Each mode depends differently on the six independent elastic moduli. We have computed these dependencies but do not present them here. The hysteresis is in the obvious direction. Our precision for these modes was five parts in 10⁶. Note that at least one mode shows clearly no changes at the CDW transition, while others show varying degrees of hysteresis and discontinuity.

crystal, indicating that microstructural effects are weak or absent and marking this as one of the very few systems in which the entire elastic tensor is well defined both above and, more unusually, below a CDW transition. The adiabatic elastic tensor c_{ijkl} (Ref. 6) (in contracted Voigt notation it would be c_{ij}) (Ref. 4) is

$$c_{ijkl} = \left. \frac{\partial^2 E}{\partial \epsilon_{ij} \partial \epsilon_{kl}} \right|_s, \quad (1)$$

where E is the internal energy, ϵ_{ij} are the symmetrized strains, and s is entropy. For a tetragonal-symmetry system such as Lu₅Ir₄Si₁₀, there are six independent elastic stiffnesses. If we define the *c* axis of the *P4/mbm* structure to be the unique axis, then the independent moduli⁶ are c_{11} , c_{33} , c_{23} , c_{12} , c_{44} , and c_{66} . Here c_{11} determines the longitudinal sound speed along (100) and (010) directions, c_{33} determines the longitudinal sound speed along the *c* axis (001), c_{66} controls the shear sound speed along (100) or (010) with displacements parallel to the *a-b* plane (and vice versa), c_{44} controls the shear-wave speed along the *c*-axis with displacements along (100) or (010) (and vice versa), and c_{23} , c_{12} along with c_{11} , c_{33} determine the Young's moduli. Accordingly, knowledge of the complete elastic tensor can provide detailed information about the internal energy, free energy, bond angle and length changes at a phase transition.¹³ In Fig. 2 we show the variation of several of the 25 or so resonance frequencies used to determine the six moduli across the CDW transition, while in Table I we list all the moduli just above and just below the CDW transition.

We observed no features whatsoever near the superconducting transition temperature T_c . In contrast, we found substantial changes near T_{CDW} , shown in the overall scan for

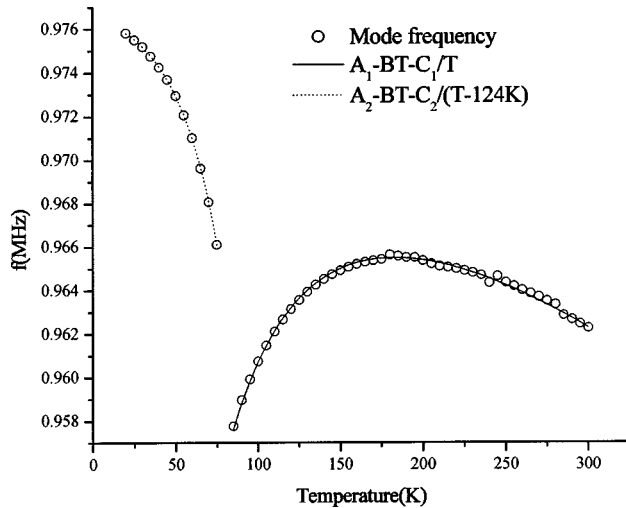


FIG. 3. A primarily c_{11} mode showing a fit to the Curie behavior above T_{CDW} and a Curie-Weiss behavior below. The fit included a constant background, and a background varying linearly with T to account for thermal expansion. The linear background was the same for the data above the CDW transition as for below. The Curie-Weiss constant for the data below T_{CDW} is $124 \text{ K} \pm 4 \text{ K}$, while above it is $0 \pm 5 \text{ K}$.

one representative mode in Fig. 3, where we show data for a mode that is 94% dependent on c_{11} . Following Landau theory for a structural phase transition,^{6,10} fits to Curie (above T_{CDW}) and Curie-Weiss (below T_{CDW}) behaviors are shown. The fits include a Curie/Curie-Weiss component, a constant background, and a component that varied linearly with T to account for thermal expansion. The slope of the linear component was the same above and below T_{CDW} . We expect different Curie-Weiss constants above and below T_{CDW} because on undergoing a first order phase transition, the system loses “memory” of how the temperature dependences of the susceptibilities behaved on the opposite side of the phase transition.¹⁴ Therefore, there is no real constraint that the Curie-Weiss constant describing the temperature dependence of susceptibilities be either non-zero or the same as the temperature at which the first-order phase transition occurs. Thus a Curie-Weiss constant of 124 K, far above T_{CDW} , is consistent with mean field theory for a first-order transition. We note further that the elastic moduli (the inverse mechanical susceptibilities) could be Curie-Weiss in the mean-field limit at either a second-order or a weak-first-order transition.¹⁴ However, in a second-order transition the c_{ij}

must exhibit a step discontinuity downward on cooling¹⁰ if the order parameter Φ is coupled to the strains quadratically (a first-order transition can also display this behavior). That is, if F_c is the free-energy term coupling strain to order parameter, then we expect

$$F_c \propto \epsilon_{ij} \phi^2 \quad (2)$$

because it should not matter whether the CDW distortion is shifted by a half wavelength (a simple phase shift is equivalent to a sign reversal in Φ). Nevertheless, hysteresis and a step discontinuity upward, seen in Fig. 2, can only occur for first order transitions. What is unusual about the elastic response to the CDW is that key changes in moduli (c_{11} , c_{66}) are associated with the a - b plane, not the c axis (c_{33} , c_{44} are sensitive to changes along c). The c axis is, however, the direction reported³ for the CDW \mathbf{q} (propagation) vector. Thus it appears that the CDW must derive most of the changes by assembling them from quasi-continuous lateral charge transfer in the a - b plane. When the lateral charge transfer reaches a critical value, charge propagation develops in the c direction. This helps to understand why c_{33} exhibits an apparent first-order transition but c_{11} shows apparent second-order behavior. We can further understand this by noting that a first-order transition represents a perturbation of a second-order one, and that the thermodynamics is anisotropic. This is illustrated by Testardi’s thermodynamic model,¹² which shows that changes in moduli are proportional to $[d \ln(T_c)/d\sigma_{ij}]^2$ where σ_{ij} denotes stress, clearly anisotropic for $\text{Lu}_5\text{Ir}_4\text{Si}_{10}$ because of the crystal structure. Oxide superconductors show similar behavior.¹⁵

In conclusion, with measurements of the fourth-rank elastic modulus tensor presented here, coupled with previous studies of the second-rank thermal expansion tensor and scalar specific heat,³ $\text{Lu}_5\text{Ir}_4\text{Si}_{10}$ becomes perhaps the best characterized commensurate CDW from a thermodynamic standpoint. Such a complete suite of measurements provides unmistakable evidence of a weak first-order transition, as well as quantities (c_{ij}) that are directly calculable from electronic structure theory, so that theoretical models can be precisely constrained.

ACKNOWLEDGMENTS

Part of this work was performed under the auspices of the U.S. Department of Energy, the National Science Foundation, and the National High Magnetic Field Laboratory.

¹H. F. Braun, K. Yvon, and R. Braun, *Acta Crystallogr., Sect. B: Struct. Crystallogr. Cryst. Chem.* **36**, 2397 (1980).

²H. D. Yang, R. N. Shelton, and H. F. Braun, *Phys. Rev. B* **33**, 5062 (1986); R. N. Shelton, L. S. Hausermann-Berg, P. Klavins, H. D. Yang, M. S. Anderson, and C. A. Swenson, *ibid.* **34**, 4590 (1986).

³B. Becker, N. G. Patil, S. Ramakrishnan, A. A. Menovsky, G. J. Nieuwenhuys, and J. A. Mydosh, *Phys. Rev. B* **59**, 7266 (1999);

B. Becker, Ph.D. Thesis, Leiden University, 1998.

⁴A. M. Gabovich, A. I. Voitenko, J. F. Annett, and M. Ausloos, *Supercond. Sci. Technol.* **14**, R1 (2001).

⁵Quasar International, Inc., 2704 Yale Blvd., SE, Albuquerque, NM 87106 or DRS, Lane 13, Powell, WY.

⁶A. Migliori, J. L. Sarrao, William M. Visscher, T. M. Bell, Ming Lei, Z. Fisk, and R. G. Leisure, *Physica B* **1**, 183 (1993).

⁷R. Peierls, *Quantum Theory of Solids* (Oxford, Clarendon, 1965),

- Sec. 5.3.
- ⁸L. Landau, *Phys. Z. Sowjetunion* **11**, 26 (1937).
- ⁹L. D. Landau, in *Collected Papers of L.D. Landau* (Pergamon, Oxford, 1965), p. 193.
- ¹⁰L. D. Landau and E. Lifshitz, *Statistical Physics* (Pergamon, Oxford, 1980), Chap. XIV, p. 451.
- ¹¹H. Ledbetter, S. Lin, and S. Kim, “Landau Theory of Phase Transitions and Tricritical Points in a Magnetic System,” NIST, Boulder (2002), unpublished results. Available from author.
- ¹²L. Testardi, *Phys. Rev. B* **12**, 3849 (1975).
- ¹³V. Keppens and A. Migliori, in *Experimental Methods in the Physical Sciences* (Academic, San Diego, 2001), Vol. 39, p. 189.
- ¹⁴R. A. Cowley, *Adv. Phys.* **29**, 1 (1980); **29**, 42 (1980); **29**, 43 (1980).
- ¹⁵B. Golding, W. Haemmerle, L. Schneemeyer, and J. Waszczak, in *Proceedings IEEE Ultrasonics Symposium* (IEEE, New York, 1988), p. 1079.